AGU PUBLICATIONS

Geophysical Research Letters

RESEARCH LETTER
10.1002/2017GL073395

Key Points:
- Arctic winter warming events are a normal part of the Arctic winter climate. Observations of these events date back to the Fram expedition
- North Pole region typically experiences 10 distinct warming events per winter, compared with 5 in the Pacific Central Arctic
- Positive trends in the number and duration of Arctic winter warming events (1980–2016), with strongest trends for North Pole domain

Supporting Information:
- Supporting Information S1

Correspondence to:
R. M. Graham,
robert.graham@npolar.no

Citation:
Graham, R. M., L. Cohen, A. A. Petty, L. N. Boisvert, A. Rinke, S. R. Hudson, M. Nicolaus, and M. A. Granskog (2017), Increasing frequency and duration of Arctic winter warming events, *Geophys. Res. Lett.*, *44*, 6974–6983, doi:10.1002/2017GL073395.

Received 9 MAR 2017
Accepted 12 MAY 2017
Published online 10 JUL 2017

Increasing frequency and duration of Arctic winter warming events

Robert M. Graham[1], Lana Cohen[1], Alek A. Petty[2,3], Linette N. Boisvert[2,3], Annette Rinke[4], Stephen R. Hudson[1], Marcel Nicolaus[5], and Mats A. Granskog[1]

[1]Norwegian Polar Institute, Tromsø, Norway, [2]Cryospheric Sciences Laboratory, Earth System Science Interdisciplinary Center, University of Maryland, College Park, Maryland, USA, [3]Goddard Space Flight Center, National Aeronautics and Space Administration, Greenbelt, Maryland, USA, [4]Alfred Wegener Institute, Helmholtz Centre for Polar and Marine Research, Potsdam, Germany, [5]Alfred Wegener Institute, Helmholtz Centre for Polar and Marine Research, Bremerhaven, Germany

Abstract Near-surface air temperatures close to 0°C were observed in situ over sea ice in the central Arctic during the last three winter seasons. Here we use in situ winter (December–March) temperature observations, such as those from Soviet North Pole drifting stations and ocean buoys, to determine how common Arctic winter warming events are. Observations of winter warming events exist over most of the Arctic Basin. Temperatures exceeding −5°C were observed during >30% of winters from 1954 to 2010 by North Pole drifting stations or ocean buoys. Using the ERA-Interim record (1979–2016), we show that the North Pole (NP) region typically experiences 10 warming events (T2m > −10°C) per winter, compared with only five in the Pacific Central Arctic (PCA). There is a positive trend in the overall duration of winter warming events for both the NP region (4.25 days/decade) and PCA (1.16 days/decade), due to an increased number of events of longer duration.

Plain Language Summary During the last three winter seasons, extreme warming events were observed over sea ice in the central Arctic Ocean. Each of these warming events were associated with temperatures close to or above 0°C, which lasted for between 1 and 3 days. Typically temperatures in the Arctic at this time of year are below −30°C. Here we study past temperature observations in the Arctic to investigate how common winter warming events are. We use time temperature observations from expeditions such as Fram (1893–1896) and manned Soviet North Pole drifting ice stations from 1937 to 1991. These historic temperature records show that winter warming events have been observed over most of the Arctic Ocean. Despite a thin network of observation sites, winter time temperatures above −5°C were directly observed approximately once every 3 years in the central Arctic Ocean between 1954 and 2010. Winter warming events are associated with storm systems originating in either the Atlantic or Pacific Oceans. Twice as many warming events originate from the Atlantic Ocean compared with the Pacific. These storms often penetrate across the North Pole. While observations of winter warming events date back to 1896, we find an increasing number of winter warming events in recent years.

1. Introduction

Temperatures in the Arctic are increasing twice as fast as the global average [*Serreze and Francis*, 2006; *Graversen et al*., 2008; *Serreze and Barry*, 2011]. The most rapid Arctic warming has been recorded during the winter months [*Graversen et al*., 2008; *Bekryaev et al*., 2010; *Boisvert and Stroeve*, 2015], and 2015–2016 was the warmest winter since records began in 1950 [*Cullather et al.*, 2016b; *Overland and Wang*, 2016]. Winter 2015–2016 featured an Arctic wide (north of 66°N) winter temperature anomaly of approximately 5°C, which was 2°C warmer than the previous record [*Overland and Wang*, 2016]. The winter maximum sea ice extent in March 2017 was the lowest in the 38 year satellite record (http://nsidc.org/arcticseaicenews/). March 2016 and March 2015 were the joint lowest, prior to 2017 [*Perovich et al.*, 2016].

In late December 2015, there was widespread media attention following observations that near-surface air temperatures close the North Pole increased to approximately 0°C during midwinter [*Boisvert et al.*, 2016; *Moore*, 2016]. These extreme temperatures were observed in situ by several Snow Buoys [*Grosfeld et al.*, 2016]. Data from these buoys were transmitted in near real time via the Global Telecommunication System (GTS), for assimilation into weather forecast models, and the anomalous temperatures were rapidly reported by the press. During this event, temperatures exceeded −10°C for between 1 and 2 days (Figure 1a). This type

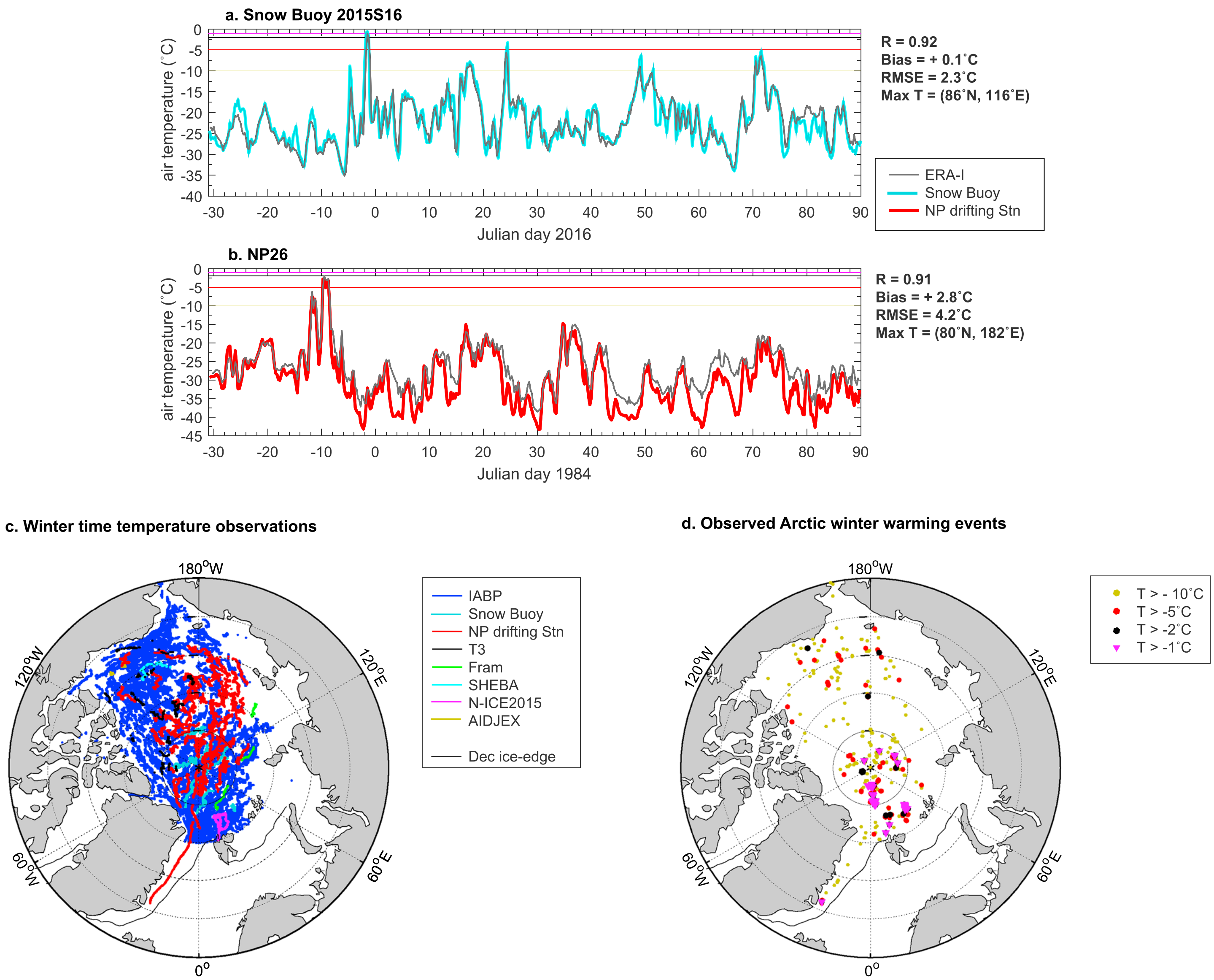

Figure 1. Time series of mean six-hourly near-surface air temperature from (a) Snow Buoy 2015S16 and (b) NP26 compared with ERA-I, nearest grid point mean six-hourly 2 m temperature. (c) Location of in situ winter time (December–March) surface air temperature observations in the Arctic (see supporting information and Table S1 for further details of data included). (d) Location of in situ observations of Arctic winter warming events. Yellow dots indicate warming events with a maximum temperature greater than −10°C. Red dots indicate temperatures greater than −5°C. Black dots indicate temperatures greater than −2°C. Pink triangles indicate temperatures greater than −1°C. Temperature thresholds are also indicated in Figures 1a and 1b using same colors. Mean ice edge (0.15 concentration) for December 2006–2015 from ERA-I is indicated by a thin black line. December ice edge is shown as this is the smallest ice extent for winter months, and the most recent 10 year period is chosen to reflect the recent ice retreat.

of event is estimated to occur between once and twice per decade [*Moore*, 2016]. However, this estimate is based on analyses that are limited to the month of December and for the North Pole region, rather than the wider Arctic Basin and full winter season [*Moore*, 2016]. Similar events with positive temperatures north of 85°N were observed in situ by Snow Buoys again during December 2016 and February 2017 (Figure S1 in the supporting information).

Recent studies have used a combination of satellite data, atmospheric reanalyses, and buoy data to investigate the synoptic conditions leading up to the 2015–2016 winter warming event(s) [*Boisvert et al.*, 2016; *Cullather et al.*, 2016b; *Moore*, 2016; *Overland and Wang*, 2016; *Kim et al.*, 2017]. The record warmth during winter 2015–2016, as a whole, has been attributed to a split tropospheric vortex [*Overland and Wang*, 2016].

This drove persistent southerly flow from the Atlantic Ocean toward the North Pole, bringing multiple storm systems and strong warm and moist air advection [*Boisvert et al*., 2016; *Cullather et al*., 2016b; *Moore*, 2016; *Overland and Wang*, 2016].

Similar to the 2015–2016 and 2016–2017 winter warming events, temperatures close to 0°C were observed on multiple occasions in an area of pack-ice north of Svalbard, from January to March 2015, during the Norwegian young sea-ice campaign (N-ICE2015) [*Graham et al*., 2017]. N-ICE2015 is one of few intensive field campaigns to span the winter season in the Arctic [*Granskog et al*., 2016], and it is the first to provide comprehensive in situ measurements of the coupled atmosphere-snow-ice-ocean system during multiple "extreme" winter warming events [*Graham et al*., 2017; *Kayser et al*., 2017; *Meyer et al*., 2017; *Provost et al*., 2017; *Walden et al*., 2017]. During these events, temperatures greater than −10°C typically lasted between 1 and 3 days, and the maximum temperatures observed were up to 30°C warmer than those before and after the event (Figure S2). Each of the warming events observed during N-ICE2015, and the following winters, were associated with major storms entering the Arctic [*Moore*, 2016; *Cohen et al*., 2017].

One of the most valuable meteorological data sets for the Arctic Ocean is derived from observations made by manned Soviet North Pole drifting stations, led by the Arctic and Antarctic Research Institute in St Petersburg. These data are highly valuable due to the spatial and temporal coverage. The data set extends back to 1937, and at least one station was in operation every year from 1954 to 1991. These near-surface air temperature and mean sea level pressure data are also valuable for their accuracy and have been used as a benchmark for the growing number of autonomous buoys that have been deployed as part of the International Arctic Buoy Program (IABP) from 1979 onward [*Rigor et al*., 2000]. Together, the drifting station and IABP observations have the best spatial and temporal coverage of any in situ meteorological data sets from the Arctic Ocean and importantly include data from the winter season [*Rigor et al*., 2000]. These data have been used to produce regional climatologies for the Arctic and to study seasonal trends and variability in near-surface air temperatures [*Rigor et al*., 2000; *Polyakov et al*., 2003].

A small number of intensive field campaigns have spanned a single winter season in the Arctic, collecting more comprehensive measurements compared with ocean buoys, such as cloud properties and radiative fluxes. Examples are the N-ICE2015 [*Granskog et al*., 2016], the Surface Heat Budget of the Arctic Ocean (SHEBA) campaign in the Beaufort Sea during the winter of 1997–1998 [*Perovich et al*., 1999], and the 2007–2008 International Polar Year—Circumpolar Flaw Lead study in the Canadian Archipelago [*Barber et al*., 2010]. Atmospheric measurements from these three campaigns have revealed two distinct Arctic winter states: the cold radiatively clear state and the warmer opaquely cloudy state [*Stramler et al*., 2011; *Raddatz et al*., 2015; *Graham et al*., 2017; *Persson et al*., 2016]. Opaquely cloudy conditions are triggered by synoptic events entering the Arctic, which cause an inward flux of heat and moisture and the development of mixed phase clouds [*Morrison et al*., 2011; *Stramler et al*., 2011; *Pithan et al*., 2014; *Graham et al*., 2017; *Persson et al*., 2016]. These conditions typically last on the order of a few days. Each winter warming event observed during N-ICE2015 was associated with opaquely cloudy conditions [*Graham et al*., 2017]. As a consequence of the two winter states, the Arctic has a bimodal surface temperature distribution for the winter months. This means that at most times and locations within the Arctic during winter, the surface air temperature will either be significantly (approximately 10°C) above or below the seasonal mean temperature.

In this study, we will place the recent "extreme" Arctic winter warming events from 2015, 2016, and 2017 into a historical context. In particular, we analyze in situ winter time near-surface air temperature observations and the ERA-Interim reanalysis (ERA-I) to explore both where and how frequently winter warming events occur across the central Arctic. We further investigate trends in the maximum temperatures recorded during warming events, as well as the frequency and duration of these events, over the ERA-I record (1979–2016).

2. Data

For this study, we use in situ winter time (December–March (DJFM)) near-surface air temperature observations from ice covered regions of the Arctic Ocean. These in situ data span more than a century (Table S1). Some of the campaign data we utilize span several years, and continue over the summer months from spring till fall. However, we only consider the winter data. The stations' locations all follow the drift of the sea ice (Figure 1c). Therefore most locations are only sampled at one point in time. During some winters no in situ data are available, while in other years several ice stations or buoys have been in operation simultaneously, and thus recorded the same winter warming event at more than one location (Figure 1, Table S1). These important factors must be taken into consideration when interpreting the data.

One of the main data sets we use in this study is the Arctic Meteorology and Climate Atlas [*Arctic Climatology Project, Environmental Working Group*, 2000]. This includes three- to six-hourly mean near-surface air temperatures from Soviet North Pole manned drifting ice-stations NP01-NP31, which were in operation from 1937–1991 (Figure 1, Table S1). Other data included in the Atlas are temperature measurements from the Fram expedition (1893–1896), the Arctic Ice Dynamics Joint Experiment (AIDJEX, 1975–1976), and the T-3 ice station that was in operation between 1952 and 1971. We further include data from SHEBA [*Perovich et al.*, 1999; *Persson*, 2011], N-ICE2015 [*Hudson et al.*, 2015; *Cohen et al.*, 2017], as well as eight Snow Buoys that observed the 2015–2016 winter warming event close to the North Pole, which were deployed by the Polarstern on the expedition PS94 in September 2015 [*Grosfeld et al.*, 2016; Table S1].

The second major data set we use is mean three-hourly near-surface air temperature observations from the IABP, covering the period 1979–2010 [*Rigor et al.*, 2000]. Approximately 25 autonomous buoys were in operation at any given time over this period (Figure 1c). These data are considered somewhat less reliable than those listed above, as the unmanned instruments are susceptible to issues such as frosting, snow build up and blowing over. Data cleaning methods are described in the supplementary material.

The height above the surface of the temperature observations used in this study varies between 1 m and 2.5 m for the different data sources, and is dependent on snow accumulation. Similarly, the temporal resolution of the data varies from 1 to 6 h. Some of the older observations may be instantaneous temperature readings, but most are temporal averages. See Supplementary Information and Table S1 for further information about the different data used.

We further utilize the ERA-I atmospheric reanalysis [*Dee et al.*, 2011]. Specifically, we use DJFM six-hourly mean 2 m temperature fields from 1979–2016. Many meteorological observations, and satellite data, around the globe are assimilated into ERA-I [*Dee et al.*, 2011]. However, there are relatively few consistent meteorological observations in the central Arctic compared with land areas and lower latitudes, particularly during winter months and earlier years of ERA-I [*Cullather et al.*, 2016a]. This somewhat reduces confidence in the state estimates produced by reanalyses for the Arctic. It is important to note that the ERA-I record does not coincide with the same time interval that the in situ data span. Of the in situ observations used from the Arctic Meteorology and Climate Atlas, 70% were made prior to 1979 and thus predate ERA-I.

3. Results

3.1. In Situ Observations of Winter Warming Events

We define Arctic winter warming events here as any time period when the near-surface (1–2.5 m) air temperature rises above −10°C, over sea ice covered regions in the Arctic Ocean during winter months (DJFM). This threshold value represents a departure of approximately 15°C from the regional mean Arctic winter temperature (1979–2016), based on ERA-I. We further study the occurrence of more "extreme" winter warming events that cross the threshold temperatures of −5°C, −2°C, and −1°C (Figures 1a and 1b). The choice of these thresholds is somewhat arbitrary but does not significantly alter any of the conclusions drawn from this study.

Arctic winter warming events have been observed in situ at locations over most of the Arctic Basin for more than a century (Figure 1). For example, a temperature of −3.7°C was observed at 84°N in March 1896, during the Fram expedition (Table S1). The Atlantic sector of the Arctic Ocean has the highest clustering of observed winter warming events (Figure 1d). Many of these observations are located north of 85°N, and there are several events where observed near-surface temperatures were greater than −1°C. For example, in February 1956 NP05 recorded a temperature of −0.4°C at 86°N (Table S1). There are also widespread observations of winter warmings greater than −5°C in the Pacific sector of the Arctic Ocean up to 80°N (Figure 1d). For example, in December 1983 NP26 observed a near-surface temperature of −1.3°C, just north of 80°N at 180°E (Figures 1b and S3a). There are relatively few in situ observations of winter warming events between 80°N and 85°N in the Pacific sector of the Arctic (Figure 1d).

Temperatures greater than −5°C were observed by a North Pole drifting station in more than 30% of all winters where these stations were in operation, covering the time period from 1951 to 1991 (Table S1). This figure increases to 60% for temperatures greater than −10°C. Similarly, winter warming events with temperatures greater than −5°C were observed by IABP buoys in just over 30% of the winters from 1979 to 2010 (not shown). With the exception of the 2015–2017 Snow Buoys, none of the in situ platforms analyzed here have recorded positive temperatures during winter (Figures 1, S1, and S2, Table S1).

The most frequent observations of "extreme" winter warming events (temperatures close to 0°C) are in the Atlantic sector of the Arctic Ocean, including the latitude band of 85°N around the North Pole (Figure 1d). However, these spatial patterns may partly be the result of sampling biases (i.e., this is where most in situ observations are available). In the north of Greenland and the Canadian Archipelago, there are comparatively fewer observations of winter warming events, and the majority of these events do not exceed temperatures of −5°C (Figure 1). However, there are also fewer in situ observations from these regions. There are too few observations over the Siberian Shelf to draw conclusions about this region (Figure 1).

From these analyses, we conclude that recent observations of winter temperatures near 0°C in the central Arctic are not without precedent [*Boisvert et al.*, 2016; *Cullather et al.*, 2016b; *Graham et al.*, 2017; *Moore*, 2016].

3.2. Winter Warming Events in ERA-Interim

The in situ temperature observations analyzed in section 3.1 show that winter warming events have been observed over most ice-covered regions of the Arctic Ocean (Figure 1). However, the spatial and temporal discontinuities with these in situ observations preclude a complete picture of the frequency and distribution of winter warming events across the Arctic. To achieve this, we utilize ERA-I. To assess whether ERA-I is a suitable product for this purpose, we compare in situ observations of extreme winter warming events ($T > -5$°C) that occurred from 1979 to 2016 with ERA-I (Figures 1a, 1b, and S2, Table S1). Data from the later NP drifting stations, SHEBA, N-ICE2015, and the ocean buoys are included in the GTS data archive for assimilation into ERA-I. Overall, ERA-I performs well. The temperature time series of ERA-I and the in situ observations have an average correlation of $R = 0.92$ (range 0.89–0.97) and a root mean square error between 2.3°C and 5.1°C (Figures 1a, 1b, and S2). There is a known warm bias in ERA-I for the Arctic [*Jakobson et al.*, 2012; *Wesslén et al.*, 2014]. Interestingly, this warm bias is not apparent when comparing ERA-I with data from the Snow Buoys (Figure 1). The warm bias in ERA-I is clearly confined to cold and stable periods and not warming events [Figures 1b and S2; *Graham et al.*, 2017]. Overall for the data considered here, ERA-I has a warm bias of approximately 3°C. However, if we consider only periods where the observed temperature is greater than −10°C, ERA-I has a cold bias of −0.9°C. Importantly, ERA-I accurately captures the timing and duration of warming events (Figures 1 and S2). This is perhaps unsurprising as warming events occur under strong synoptic forcing, which ERA-I is known to simulate well [*Graham et al.*, 2017]. Thus, we conclude that ERA-I is a suitable product to use for this study.

We first investigate the maximum recorded six-hourly winter time 2 m temperature for each grid cell in ERA-I, over the period 1979–2016 (Figure 2a). Winter temperatures above 0°C have been recorded in ERA-I over large areas of the Arctic Ocean. Most of the in situ observations are below the maximum recorded temperature in ERA-I (Figure 2a), which indicates that the in situ observations and ERA-I are in agreement. However, within the region north of 85°N, the warmest temperatures observed by some IABP buoys and NP06, which predates the ERA-I period, exceed the maximum temperature recorded in ERA-I by approximately 1°C (Figure 2a). The in situ observations analyzed here document a single point in time and the different locations correspond to different times that span more than a century. It is thus considered unlikely that any of the in situ measurements capture the maximum temperature experienced at any given location over the ERA-I time period.

To provide a better idea of a "typical" Arctic winter warming event, we calculate the average maximum winter temperature across the Arctic from ERA-I. Specifically, we calculate the 1980–2016 mean of the maximum six-hourly 2 m temperature recorded each winter at every grid cell (Figure 2b). We further calculate the percentage of years in ERA-I where the maximum winter six-hourly temperature exceeds −10°C, at every grid cell (Figure 2c; see supporting information Figure S4 for −5°C, −2°C, and 0°C). The most frequent occurrences of winter warming events are in the Atlantic sector of the Arctic and in the Pacific sector around the Chukchi Sea (Figure 2c). The warmest average maximum winter temperatures are also found in these regions (Figure 2b). These two pathways of winter warming events, from the Atlantic and Pacific Oceans, effectively form a bridge across the North Pole along the 0°E and 180°W meridians (Figure 2). The maximum

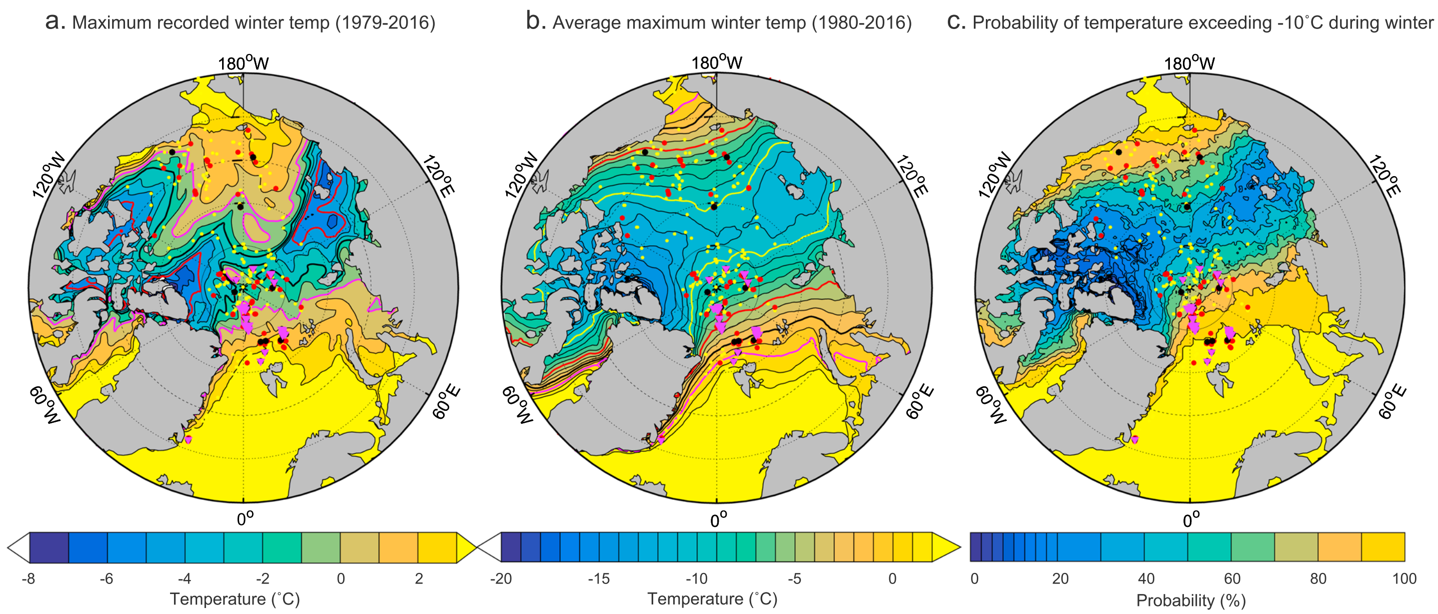

Figure 2. (a) The maximum six-hourly mean winter (December–March) 2 m temperature in ERA-Interim from 1979 to 2016. (b) The 1980–2016 average of the warmest winter six-hourly mean temperature at each grid cell. Colored contours show the 0°C isotherm (pink), −2°C isotherm (black), −5°C isotherm (red), and −10°C isotherm (yellow). (c) The percentage chance of the six-hourly 2 m temperature exceeding −10°C during a given winter. Colored dots correspond to the in situ observations of winter warming events shown in Figure 1b. Yellow: T2m > −10°C. Red: T2m > −5°C. Black: T2m > −2°C. Pink: T2m > −1°C.

temperature exceeds −10°C in more than 75% of winters at the North Pole and −5°C in 25% of winters (Figures 2c and S4a). Winter warming events originating in the Pacific sector of the Arctic typically do not penetrate to as high latitudes as those from the Atlantic, although they still penetrate great distances into the Arctic (Figures 2 and S3). For example, in the Atlantic sector, the average maximum winter temperature is −4°C at 85°N (Figure 2b). In contrast, the average maximum winter temperature in the Pacific sector at 85°N is −11°C. At 180°W, only 33% of winters experience temperatures greater than −10°C between 80°N and 85°N (Figure 2c). The reason for this asymmetry is thought to be partly due to the larger distance to open water in the Pacific sector compared with the Atlantic [*Moore*, 2016] but also the more active storm track originating from the Atlantic Ocean [*Zhang et al.*, 2004]. The closer presence of open water to the Atlantic sector results in strong temperature gradients in this region and more baroclinicity. The lowest average maximum winter temperatures are found just north of Ellesmere Island (−15°C) and on the Siberian Shelf at the boundary between the Laptev and East Siberian Sea (−12°C). In these areas, temperatures exceed −10°C in less than 10% of winters (Figures 2b and 2c).

Spatial and temporal disparities between the in situ observations and ERA-I preclude a more rigorous comparison of spatial patterns of winter warming events for the two data sets. However, there is good agreement between the regional patterns evident in ERA-I and the in situ observations (Figure 2). For example, in the regions where ERA-I shows fewer occurrences of winter warming events with temperatures above −10°C, there are fewer in situ observations of winter warming events (Figure 2c). Similarly, ERA-I shows more frequent winter warming events and higher maximum temperatures occurring in the Atlantic sector of the Arctic Ocean, where there are more in situ temperature observations exceeding −1°C (Figure 2).

3.3. Frequency of Arctic Winter Warming Events and Trends in ERA-I

We further examine the net duration of warming events for each winter in ERA-I. We do this by plotting time series of the total time each winter where the mean six-hourly temperature exceeds a given threshold anywhere in two specified domains, such that 1 day corresponds to 4 × (not necessarily consecutive) 6 h time steps. These thresholds are taken to be −10°C, −5°C, −2°C, and 0°C. We chose two domain areas for these analyses: north of 85°N and the region between 75°N–80°N and 150°E–138°W (Figure 3a). Both domains are of broadly equal area, and we shall refer to these as the North Pole (NP) and Pacific Central Arctic (PCA) domains, respectively. These two domains have been chosen as they are primarily influenced by

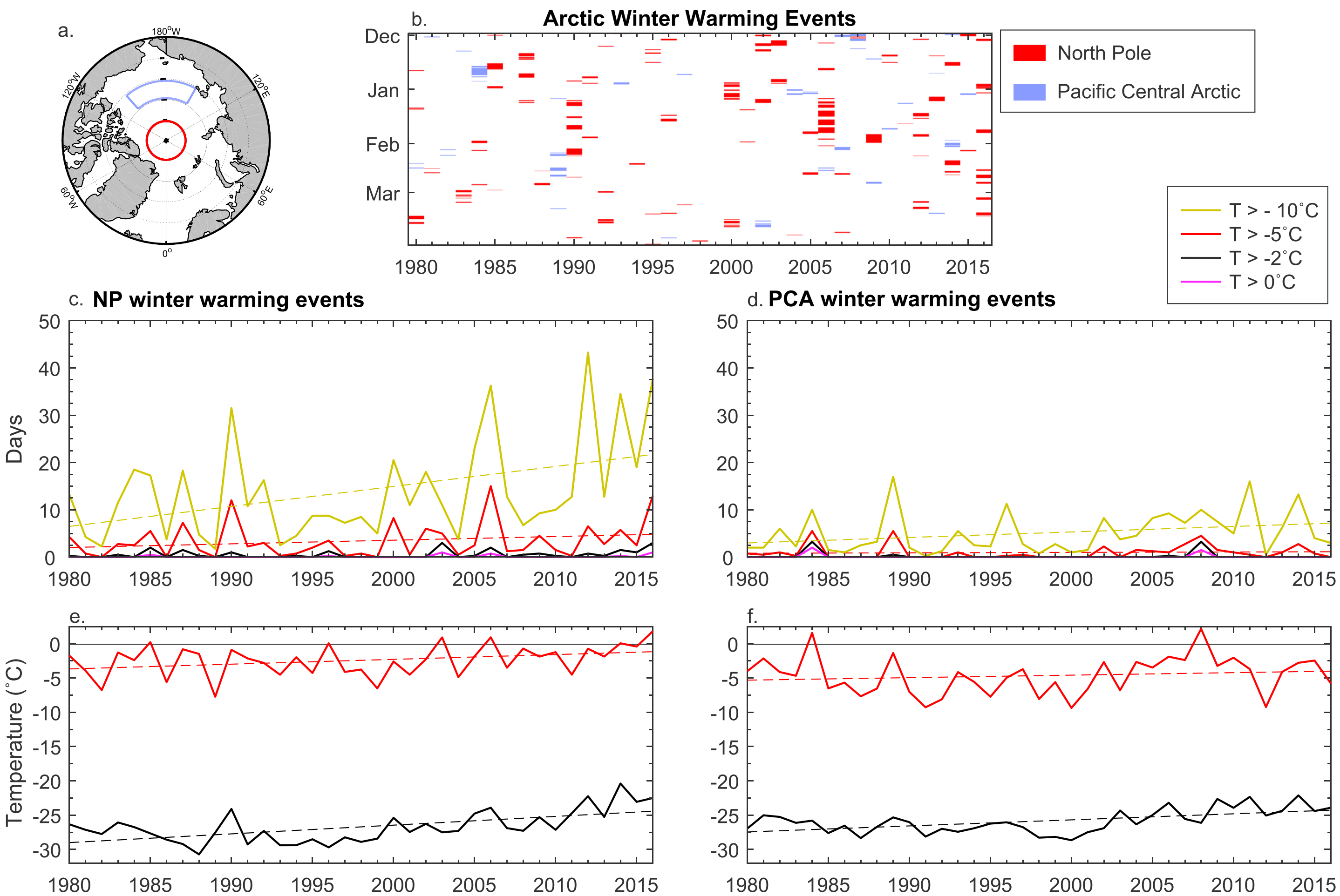

Figure 3. (a) Location of North Pole (NP) and Pacific Central Arctic (PCA) domains. (b) Timing of winter warming events with a 2 m temperature greater than −5°C for the NP (red) and PCA (blue) domains, from 1980 to 2016 in ERA-I. Note that December always corresponds to the preceding year, such that December 1979 is considered winter 1980, etc. Total time each winter where the maximum 2 m temperature anywhere within the (c) NP and (d) PCA domains exceeds the stated threshold (see legend). Maximum (red) and mean (black) winter 2 m temperature for the (e) NP and (f) PCA domains. Dashed lines indicate linear trends.

winter warming events originating from the Atlantic and Pacific sectors, respectively (Figures 2 and 3a). We further plot the times each winter when the temperature exceeded the −5°C threshold at any grid point in our NP and PCA domains (Figure 3b). This provides information regarding both the number and duration of individual warming events for each domain as well as which months are associated with the largest number of events.

There is large inter-annual variability in the net duration of winter warming events, both for the NP and PCA domains (Figures 3b–3d). In some winters there is less than 24 h where the temperature is above −10°C, while in other years they total more than 40 days (out of 120). Overall, there are approximately twice as many distinct winter warming events in the NP domain (10 events) compared with the PCA (five events), and events in the NP domain typically have a longer average duration (Figure S5). As a result, there are approximately three times as many days in the NP domain where the temperature exceeds −10°C, compared with the PCA (Figures 3b–3d). Likewise, there are more days with temperatures greater than 0°C in the NP Domain (Figures 3c–3f). There were less days with temperatures greater than −5°C in both domains from 1991 to 1999, compared with the 1980s and after 2000 (Figures 3c and 3d).

Winter warming events in the NP and PCA domains rarely coincide nor do they occur in quick succession (Figure 3b). This demonstrates that winter warming events are usually regional, rather than pan-Arctic (Figures 2 and S3). Nonetheless, in December 2007, a large winter warming event brought extreme temperatures to our PCA and NP Domains, simultaneously (Figures 3b and S3c). This event originated in the Pacific sector, following a record low September sea ice extent and was associated with an unusually large area of open water North of Alaska for December (Figure S3c).

We further investigate inter-annual variability in the maximum temperature each winter for both the NP and PCA Domains. Maximum winter temperatures range from −9°C to +2°C in the PCA Domain and from −8°C to +2°C in the NP Domain (Figures 3e and 3f). These maximum temperatures are consistent with observations made by Snow Buoys from 2015 to 2017 (Figures 1 and S1, Table S1). The maximum winter temperature recorded in both domains is typically more than 20°C higher than the mean winter temperature. There is a positive trend in the mean winter temperature for both the NP (+1.27°C/decade) and PCA (+0.88°C/decade) domains (Figures 3e and 3f). The trend in the maximum winter temperature is smaller compared with the mean winter trend for both domains, at +0.70°C/decade for the NP and +0.37°C/decade for the PCA domain (Figures 3e and 3f), but brings the maximum winter temperature closer toward 0°C (Figures 3e and 3f). The presence of sea ice typically limits near-surface temperatures to approximately 0°C.

Using the JRA55 reanalysis, *Moore* [2016] found that the positive trend in the maximum (99th percentile) December 2 m air temperature for the North Pole region was twice as strong as the mean 2 m air temperature trend. With ERA-I, we find a much larger positive trend for the maximum temperature in the month of December (+1.80°C/decade), compared with the overall winter trend for the maximum winter temperature (+0.70°C/decade), in our NP domain. In contrast, there is a small negative trend for the month of March. These results suggest that it is becoming more common to have at least one "extreme" winter warming occurring during the month of December in the NP domain. We do not find evidence of a large increase in the maximum temperature of winter warming events. For our PCA domain, the largest trend in ERA-I for the maximum temperature realized in a single month is January (+1.19°C/decade), and the smallest is February (−0.01°C/decade).

We find a positive trend in the net duration of winter warming events for both the NP and PCA domains (Figures 3c and 3d). For winter warming events greater than −10°C, this trend amounts to 4.25 days/decade for the NP domain and 1.16 days/decade for the PCA domain. These trends are due to an increase in the number of distinct winter warming events (1.7 events/decade for NP and 0.6 events/decade for the PCA domain), as well as an increase in the average duration of an individual event (+5 h/decade NP and +4 h/decade PCA; Figure S5). The positive trend in the maximum duration of a single winter warming event (+24 h/decade NP, and +12 h/decade PCA, Figure S5) is much larger than that of the average duration. Nonetheless, there is large variability in the length of winter warming events within a single season, as well as interannual variability in the number and average length of events (Figures 3 and S5).

4. Summary

We have analyzed in situ Arctic near-surface air temperature observations from winter (December–March) to find evidence of past Arctic winter warming events. In situ observations of Arctic winter warming events date back to the Fram expedition in 1896 and have since been recorded across much of the Arctic Basin. Winter temperatures greater than −1°C have been observed in situ north of 85°N as early as 1956. Despite a sparse observation network, temperatures greater than −5°C were observed during more than 30% of all winters from 1954–2010 by either North Pole drifting stations or IABP buoys. These results suggest that in situ observations of temperatures near 0°C in the central Arctic during the last three winter seasons are not unprecedented.

When compared with in situ observations, the ERA-I reanalysis is found to reproduce the timing and duration of winter warming events well. We use ERA-I to investigate the spatial occurrences of Arctic winter warming events, and the frequency of these events. The patterns revealed by ERA-I and the in situ observations are in good agreement. The highest occurrences of winter warmings are found in the Atlantic sector of the Arctic Ocean. Winter warming events originating from the Atlantic sector frequently penetrate across the North Pole within the latitude circle of 85°N. Arctic winter warming events also originate from the Pacific sector, namely through the Chukchi Sea. Warming events in the Pacific sector typically do not penetrate to as high latitudes as events originating from the Atlantic, but large winter warming events with positive temperatures do still occur in the Pacific sector. The lowest occurrences of winter warming events are north of Greenland, the Canadian Archipelago, and on the Siberian Shelf.

There is large interannual variability in the number and duration of Arctic winter warming events (T2m $> -10°C$) originating from both the Atlantic and Pacific sectors. Overall, there are approximately 10 distinct warming events each winter in our North Pole domain and five in the Pacific Central Arctic. Winter warming events in the North Pole domain typically have a longer average duration compared with the Pacific Central Arctic. There is a positive trend from 1980 to 2016 in the maximum winter 2 m air temperature (0.70°C/decade) at the North Pole, but this is smaller than the mean winter trend (1.27°C/decade). We do not find evidence of a rapid increase in the maximum temperature of winter warming events. This is because the maximum near-surface temperature is limited to approximately 0°C while sea ice is present, and winter warming events already frequently approach this limit.

Together with the positive trend in the maximum temperature of winter warming events, we find a positive trend in the net duration of winter warming events in both of our domains. This trend totals 4.25 days/decade for the North Pole domain and 1.16 days/decade in the Pacific Central Arctic domain, for ERA-I. These trends are due to an increased number of distinct winter warming events and an increase in the average length of a single event. These patterns are consistent with recent studies that have indicated part of the rapid rise in Arctic winter temperatures may be linked to the increased occurrence of winter storm events or moisture intrusions, which transport warm and moist air into the Arctic from the midlatitudes [*Park et al.*, 2015; *Boisvert et al.*, 2016; *Graham et al.*, 2017; *Woods and Caballero*, 2016].

Acknowledgments
This work has been funded through the Norwegian Polar Institute's Centre for Ice, Climate and Ecosystems (ICE) through the N-ICE project. This work has been further supported by the German Academic Exchange Service (DAAD) and PPP Norway. The Arktis 2030 program of the Ministries of Foreign Affairs and Climate and Environment of Norway, through the project ID Arctic, supported L.C. L.B. and A.P. are funded through NASA's Operation IceBridge Project Science Office. A.R. acknowledges support of the project SFB/TR172 "Arctic Amplification: Climate Relevant Atmospheric and Surface Processes, and Feedback Mechanisms (AC)^3" funded by the Deutsche Forschungsgemeinschaft (DFG) and the Helmholtz Climate Initiative REKLIM. The Arctic Meteorology and Climate Atlas is available from https://nsidc.org/data/g01938. N-ICE2015 data are available through https://data.npolar.no/dataset/7f7e56d0-9e70-4363-b37d-17915e09a935. SHEBA data are available at https://data.eol.ucar.edu/dataset/list?project=73. IABP data are available from http://iabp.apl.washington.edu/data.html. Snow Buoy data are available from http://www.meereisportal.de (grant REKLIM-2013-04). ERA-I is available from http://www.ecmwf.int/en/research/climate-reanalysis/era-interim. The authors also thank an anonymous reviewer and Julienne Stroeve for their helpful suggestions.

References

Arctic Climatology Project, Environmental Working Group (2000), *Environmental Working Group Arctic Meteorology and Climate Atlas*, edited by F. Fetterer and V. F. Radionov. Version 1., NSIDC: National Snow and Ice Data Center, Boulder, Colo., doi:10.7265/N5MS3QNJ.

Barber, D. G., M. G. Asplin, Y. Gratton, J. V. Lukovich, R. J. Galley, R. L. Raddatz, and D. Leitch (2010), The International Polar Year (IPY) Circumpolar Flaw Lead (CFL) system study: Overview and the physical system, *Atmos. Ocean*, *48*(4), 225–243, doi:10.3137/OC317.2010.

Bekryaev, R. V., I. V. Polyakov, and V. A. Alexeev (2010), Role of polar amplification in long-term surface air temperature variations and modern arctic warming, *J. Clim.*, *23*(14), 3888–3906, doi:10.1175/2010JCLI3297.1.

Boisvert, L. N., and J. C. Stroeve (2015), The Arctic is becoming warmer and wetter as revealed by the Atmospheric Infrared Sounder, *Geophys. Res. Lett.*, *42*, 4439–4446, doi:10.1002/2015GL063775.

Boisvert, L. N., A. A. Petty, and J. C. Stroeve (2016), The impact of the extreme winter 2015/16 Arctic cyclone on the Barents–Kara seas, *Mon. Weather Rev.*, *144*(11), 4279–4287, doi:10.1175/MWR-D-16-0234.1.

Cohen, L., S. R. Hudson, V. P. Walden, R. M. Graham, M. A. Granskog (2017), Meteorological conditions in a thinner Arctic sea ice regime from winter through early summer during the Norwegian young sea ICE expedition (N-ICE2015), *J. Geophys. Res. Atmos.*, *122*, doi:10.1002/2016JD026034, in press.

Cullather, R., T. M. Hamill, D. Bromwich, X. Wu, and P. Taylor (2016a), Systematic improvements of reanalyses in the Arctic (SIRTA) - A white paper produced for the U.S. Interagency Arctic Research Policy Committee. [Available at http://www.iarpccollaborations.org/uploads/cms/documents/sirta-white-paper-final.pdf.]

Cullather, R. I., Y. Lim, L. N. Boisvert, L. Brucker, J. N. Lee, and S. M. J. Nowicki (2016b), Analysis of the warmest Arctic winter, 2015–2016, *Geophys. Res. Lett.*, *43*, 808–816, doi:10.1002/2016GL071228.

Dee, D. P., et al. (2011), The ERA-Interim reanalysis: Configuration and performance of the data assimilation system, *Q. J. R. Meteorol. Soc.*, *137*(656), 553–597, doi:10.1002/qj.828.

Graham, R. M., A. Rinke, L. Cohen, S. R. Hudson, V. P. Walden, M. A. Granskog, W. Dorn, M. Kayser, and M. Maturilli (2017), A comparison of the two Arctic atmospheric winter states observed during N-ICE2015 and SHEBA, *J. Geophys. Res. Atmos.*, *122*, doi:10.1002/2016JD025475, in press.

Granskog, M. A., P. Assmy, S. Gerland, G. Spreen, H. Steen, and L. H. Smedsrud (2016), Arctic research on thin ice: Consequences of Arctic sea ice loss, *Eos Trans. AGU*, *97*(5), 22–26, doi:10.1029/2016EO044097.

Graversen, R. G., T. Mauritsen, M. Tjernström, E. Källén, and G. Svensson (2008), Vertical structure of recent Arctic warming, *Nature*, *451*(7174), 53–56, doi:10.1038/nature06502.

Grosfeld, K., et al. (2016), Online sea-ice knowledge and data platform < www.Meereisportal.De >, *Polarforschung*, *85*, 143–155, doi:10.2312/polfor.2016.011.

Hudson, S. R., L. Cohen, and V. P. Walden (2015), *N-ICE2015 Surface Meteorology [Data set]*. Norwegian Polar Institute, Norway, doi:10.21334/npolar.2015.056a61d1

Jakobson, E., T. Vihma, T. Palo, L. Jakobson, H. Keernik, and J. Jaagus (2012), Validation of atmospheric reanalyses over the central Arctic Ocean, *Geophys. Res. Lett.*, *39*, L10802, doi:10.1029/2012GL051591.

Kayser, M., M. Maturilli, R. M. Graham, S. R. Hudson, A. Rinke, L. Cohen, J.-H. Kim, W. Moon, and M. A. Granskog (2017), Vertical thermodynamic structure of the troposphere during the Norwegian young sea ICE expedition (N-ICE2015), *J. Geophys. Res. Atmos.*, doi:10.1002/2016JD026089, in press.

Kim, B.-M., et al. (2017), Major cause of unprecedented Arctic warming in January 2016: Critical role of an Atlantic windstorm, *Sci. Rep.*, *7*, 40051, doi:10.1038/srep40051.

Meyer, A., I. Fer, A. Sundfjord, and A. K. Peterson (2017), Mixing rates and vertical heat fluxes north of Svalbard from Arctic winter to spring, *J. Geophys. Res. Oceans*, doi:10.1002/2016JC012441, in press.

Moore, G. W. K. (2016), The December 2015 North Pole warming event and the increasing occurrence of such events, *Sci. Rep.*, *6*, 39084, doi:10.1038/srep39084.

Morrison, H., G. de Boer, G. Feingold, J. Harrington, M. D. Shupe, and K. Sulia (2011), Resilience of persistent Arctic mixed-phase clouds, *Nat. Geosci.*, *5*(1), 11–17, doi:10.1038/ngeo1332.

Overland, J. E., and M. Wang (2016), Recent extreme Arctic temperatures are due to a split polar vortex, *J. Clim.*, *29*(15), 5609–5616, doi:10.1175/JCLI-D-16-0320.1.

Park, D.-S. R., S. Lee, and S. B. Feldstein (2015), Attribution of the recent winter sea-ice decline over the Atlantic sector of the Arctic Ocean, *J. Clim.*, *28*, 4027–4033, doi:10.1175/JCLI-D-15-0042.1.

Perovich, D. K., et al. (1999), Year on ice gives climate clues, *Eos Trans. AGU*, *80*(41), 481–485.

Perovich, D., W. Meier, M. Tschudi, S. Farrell, S. Gerland, S. Hendricks, T. Krumpen, and C. Haas (2016), Sea Ice [in Arctic Report Card 2016]. [Available at http://www.arctic.noaa.gov/Report-Card.]

Persson, O. (2011), SHEBA composite data observations. Version 1.0. UCAR/NCAR-Earth Observing Lab., doi:10.5065/D6PN93R6.

Persson, P. O. G., M. D. Shupe, D. Perovich, and A. Solomon (2016), Linking atmospheric synoptic transport, cloud phase, surface energy fluxes, and sea-ice growth: Observations of midwinter SHEBA conditions, *Clim. Dyn.*, doi:10.1007/s00382-016-3383-1.

Pithan, F., B. Medeiros, and T. Mauritsen (2014), Mixed-phase clouds cause climate model biases in Arctic wintertime temperature inversions, *Clim. Dyn.*, *43*(1–2), 289–303, doi:10.1007/s00382-013-1964-9.

Polyakov, I. V., R. V. Bekryaev, G. V. Alekseev, U. S. Bhatt, R. L. Colony, M. A. Johnson, A. P. Maskshtas, and D. Walsh (2003), Variability and trends of air temperature and pressure in the maritime Arctic, 1875–2000, *J. Clim.*, *16*(12), 2067–2077, doi:10.1175/1520-0442(2003)016<2067:VATOAT>2.0.CO;2.

Provost, C., N. Sennéchael, J. Miguet, P. Itkin, A. Rösel, Z. Koenig, N. Villacieros-Robineau, and M. A. Granskog (2017), Observations of flooding and snow-ICE formation in a thinner Arctic sea ICE regime during the N- ICE2015 campaign: Influence of basal ICE melt and storms, *J. Geophys. Res. Oceans*, doi:10.1002/2016JC012011, in press.

Raddatz, R. L., T. N. Papakyriakou, B. G. Else, M. G. Asplin, L. M. Candlish, R. J. Galley, and D. G. Barber (2015), Downwelling longwave radiation and atmospheric winter states in the western maritime Arctic, *Int. J. Climatol.*, *35*(9), 2339–2351, doi:10.1002/joc.4149.

Rigor, I. G., R. L. Colony, and S. Martin (2000), Variations in surface air temperature observations in the Arctic, 1979–97, *J. Clim.*, *13*, 896–914, doi:10.1175/1520-0442(2000)013<0896:VISATO>2.0.CO;2.

Serreze, M. C., and R. G. Barry (2011), Processes and impacts of Arctic amplification: A research synthesis, *Global Planet. Change*, *77*(1–2), 85–96, doi:10.1016/j.gloplacha.2011.03.004.

Serreze, M. C., and J. A. Francis (2006), The arctic amplification debate, *Clim. Change*, *76*(3–4), 241–264, doi:10.1007/s10584-005-9017-y.

Stramler, K., A. D. Del Genio, and W. B. Rossow (2011), Synoptically driven Arctic winter states, *J. Clim.*, *24*(6), 1747–1762, doi:10.1175/2010JCLI3817.1.

Walden, V. P., S. R. Hudson, L. Cohen, S. Y. Murphy, and M. A. Granskog (2017), Atmospheric components of the surface energy budget over young sea ice: Results from the N-ICE2015 campaign, *J. Geophys. Res. Atmos.*, *122*, doi:10.1002/2016JD026091, in press.

Wesslén, C., M. Tjernström, D. H. Bromwich, G. De Boer, A. M. L. Ekman, L. S. Bai, and S. H. Wang (2014), The Arctic summer atmosphere: An evaluation of reanalyses using ASCOS data, *Atmos. Chem. Phys.*, *14*(5), 2605–2624, doi:10.5194/acp-14-2605-2014.

Woods, C., and R. Caballero (2016), The role of moist intrusions in winter Arctic warming and sea ice decline, *J. Clim.*, 160314091706008, doi:10.1175/JCLI-D-15-0773.1.

Zhang, X., J. E. Walsh, J. Zhang, U. S. Bhatt, and M. Ikeda (2004), Climatology and interannual variability of Arctic cyclone activity: 1948–2002, *J. Clim.*, *17*(12), 2300–2317, doi:10.1175/1520-0442(2004)017<2300:CAIVOA>2.0.CO;2.